JOURNAL OF MATERIALS SCIENCE 23 (1988) 1923–1933

# Modelling of degradation in black copper photothermal collector coatings

A. SCHERER*, O. T. INAL, R. B. PETTIT‡
*Department of Materials and Metallurgical Engineering, New Mexico Institute of Mining and Technology, Socorro, New Mexico 87801, USA and ‡Division 1824, Sandia National Laboratories, Albuquerque, New Mexico 87185, USA*

The degradation mechanism in black copper photothermal collector coatings was investigated through the use of kinetic analysis, microstructural determinations and optical modelling. The initial structure of black copper was identified using reflection electron diffraction, scanning electron microscopy and Auger electron spectroscopy sputter profiles. These results were used to develop an optical model of the as-deposited coatings. In this model, the coatings was best described as a two-layer film. The layer next to the substrate consists of dense copper oxide with metallic copper inclusions, while the rough outer layer is modelled as copper oxide dispersed in air. A substantial decrease in the solar absorptance (from 0.96 to 0.80) of coatings exposed to temperatures above 150° C in air was found to occur within 30 min and was explained by a decrease in the surface roughness of the coatings. After longer exposures, an increase in the thickness of the oxide layer near the substrate occurs at the expense of the surface layer. Incorporating this change in the model, the optical properties after thermal ageing were predicted.

## 1. Introduction

Before the moderate and long-term optical degradation behaviour of a selective solar coating can be predicted, the degradation mechanisms occurring in the coating have to be delineated. This can be done through a degradation rate analysis which provides activation energies for the reactions occurring within the coating. However, such kinetic determinations can be unreliable if extrapolation to less severe degradation conditions is desired.

Because of the complexity of electrodeposited coatings, as well as the small structural dimensions involved, detailed information about the structure and composition of these films cannot be easily obtained. Therefore a coating "model" is developed which combines both the available structural information and various unknown parameters that are adjusted to provide a "good" fit to measured optical properties [1]. In the area of solar selective coatings, this approach has yielded only approximations to the most likely mechanisms that are providing solar selectivity [2]. A somewhat better approach involves matching changes in the optical properties measured during thermal ageing with changes predicted by the model in order to provide a verification for both the model and the degradation mechanism. This strategy was successfully applied to describe the structure and thermal degradation behaviour of electrodeposited black chrome [3]. Only after a determination of the mechanism of degradation is it possible to extrapolate confidently short-term accelerated exposure data to the long times necessary for the determination of the lifetime of photothermal solar collector coatings.

The intention of the present study is to use the latter approach to characterize, through both a microstructural analysis and on optical modelling approach, the thermal degradation phenomena occurring in black copper photothermal collector coatings. This study also investigated other environmental exposures, such as those encountered during humidity and outdoor testing, in order to provide information on the stability of this coating under realistic environments.

## 2. Experimental procedure

### 2.1. Preparation of the coatings

The oxide coatings were prepared using previously determined optimized conditions that are known to favour the formation of thermally stable copper oxide films [4, 5]. Copper sheets, 5.5 cm × 5.5 cm, were prepared by chemical polishing in a solution consisting of 25 vol % nitric, 20 vol % acetic and 55 vol % phosphoric acid at 70 to 80° C for 20 to 40 sec. Such treatment yielded very shiny, chemically clean, copper substrates.

To produce copper oxide coatings, these copper sheets were then chemically oxidized in a solution consisting of 60 g $l^{-1}$ NaOH and 20 g $l^{-1}$ $K_2S_2O_8$ at 60° C for 7.5 min. The solution was changed after every five plates to avoid degradation of the electrolyte [5]. The resulting plates exhibited solar absorptance values above 0.97. The corresponding thermal emittance was found to vary substantially among the

*Present address*: Bell Communications Research, Red Bank, New Jersey 07701, USA.

0022–2461/88 $03.00 + .12 

coatings, in agreement with previously reported behaviour of black copper coatings [6, 7], but was always below 0.5.

### 2.2. Heat treatments

Heat treatments were performed in muffle furnaces operating in the range of 150 to 250° C with a temperature accuracy and uniformity of better than ± 5° C. Several samples were exposed to temperatures of 250, 205 and 150° C. One sample was used for microstructural analysis, while the others were removed at different time intervals for optical property measurements. The heat-treatment schedule was designed such that optical property data were obtained on an equal log (time) basis. The samples heat-treated for the longest duration were removed from the furnaces after 2258 h. Periodically, the spectral reflectance properties were also measured.

Humidity testing at 150° C was also performed to investigate the combined effect of temperature and humidity on the degradation behaviour of the coatings. Optical properties were measured before and after removal from this environment at regular intervals. In addition, samples were removed and analysed for microstructural information. Finally, outdoor exposure experiments were conducted by placing a black copper coating into a flat-plate collector which was designed to simulate stagnation conditions. The coatings were removed after approximately 5000 h, analysed, and the results compared to other environmental test results.

### 2.3. Microstructural analysis

A Hitachi S-310A scanning electron microscope (SEM) was used to investigate the approximate surface morphology and to obtain thicknesses of the coatings. The surface morphology of the samples was determined both before and after heat treatment or other testing conditions. SEM micrographs were also obtained from samples used in the reflection electron diffraction (RED) studies to aid in the RED characterizations.

An RCA EMU-3G transmission electron microscope (TEM) was equipped with an electron diffraction stage placed in the position of the intermediate lens. The unit was operated at 100 and 50 kV in the transmission reflection electron diffraction mode to obtain reflection–diffraction patterns of the oxide coatings. The samples were bent slightly before being observed to improve control over the beam position. The experimental details and merits of this analysis technique have been given elsewhere [8].

## 3. Theoretical studies

### 3.1. Modelling of the optical properties

Reflectance calculations were accomplished using an iterative computer program which determined the complex Fresnel coefficients of the multilayer film. The film was subdivided into a large number of layers, each of which contained uniform but different volume fractions of particles dispersed in a matrix. These slices were then stacked on top of the substrate and the overall optical response calculated according to Rouard's method [9]. Although a very large number of slices could be used, it was found that there was no advantage in using over 50 slices in each layer. The Maxwell–Garnett effective medium theory [10] was used to determine the composite complex index of refraction of individual slices. Optical property data for each slice were provided by a subroutine which generated complex refractive index values based on the material and the assumed structure of each layer. The reflectance as a function of wavelength generated by the model was then compared to the experimental data obtained from both as-plated and degraded samples to evaluate the validity of the model.

The coatings investigated in this study consisted of structurally complex stacks. The optical properties calculated from the structural model were matched to the spectral reflectance curves by simple iteration of several structural features in the coating, such as the particle sizes, particle shapes, material gradients, etc. The sum-squared difference between the measured and the calculated spectral reflectance was evaluated at wavelengths across the solar spectrum and summed to obtain a measure of the fit. Systematic minimization of this quantity through the application of a Statistical Package for the Social Sciences (SPSS) [11] optimization scheme based on a multi-variable regression was found to be unsuccessful in accurately reproducing positions of minima and maxima in the spectral reflectance curves. Therefore this procedure was not pursued and instead qualitative visual agreement between the calculated and measured reflectance curves was utilized to determine a "best" fit.

## 4. Results

### 4.1. Optical degradation

Copper oxide coatings degrade substantially during exposures to even mild conditions of temperature or temperature and humidity. This is seen from the solar absorptance and thermal emittance ageing results shown in Figs 1a and b, respectively. During heat treatment, the thermal emittance, after an initial drop, decreased slightly with time at the lower temperatures, but increased with time at higher temperatures. On the other hand, the solar absorptance decreased uniformly with time. A significant decrease in the solar absorptance was observed within the first 30 min of exposure for temperatures of 205° C and above. Based on the data in Fig. 1a, an Arrhenius plot of the time necessary to reach a given solar absorptance value is shown in Fig. 2. Also shown for comparison is the ageing behaviour determined for several other oxides [4]. An activation energy of approximately 30 kcal $mol^{-1}$ (126 kJ $mol^{-1}$) is obtained for the solar absorptance degradation of the black copper coatings over the range studied.

Degradation in the spectral reflectance behaviour of black copper, shown in Fig. 3, results in an increase in the reflectance at long wavelengths, whereas reflectance values below 800 nm do not change significantly. Changes in the solar absorptance against heat treatment at 150° C with and without humidity are shown in Fig. 4. Humidity is seen to cause an increase in the degradation of black copper, thus reducing the time needed for a 10% reduction in the solar absorptance

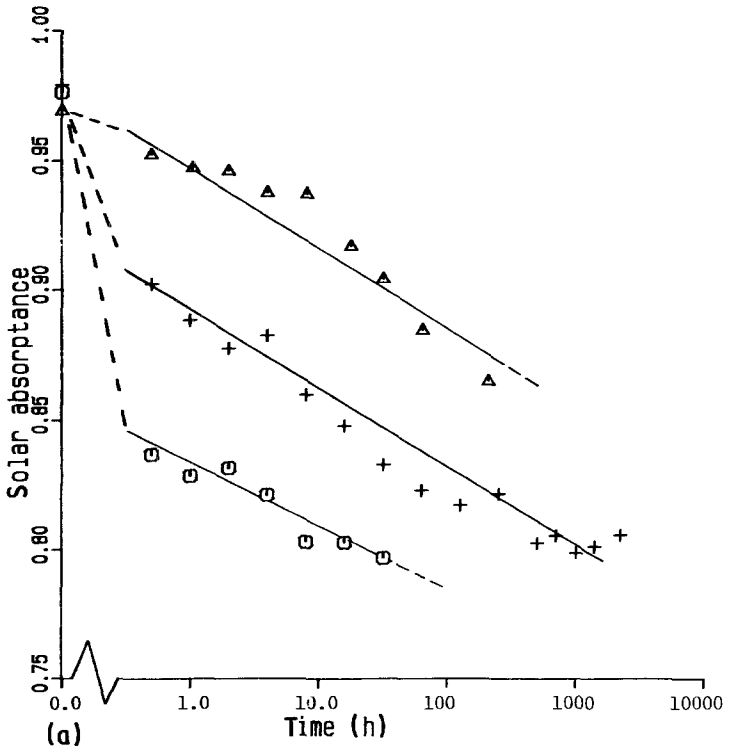


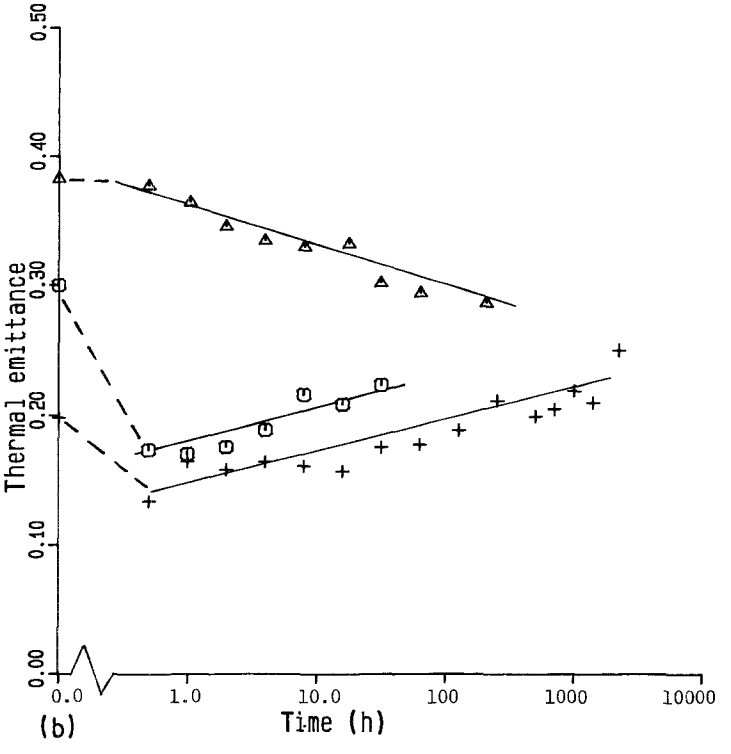


*Figure 1* (a) Solar absorptance behaviour of black copper during heat treatment at (△) 150, (+) 205, (□) 250° C. (b) Thermal emittance of black copper during heat treatment at (△) 150, (+) 205, (□) 250° C.

by approximately a factor of 6. Outdoor exposure for 156 days resulted in only a slight decrease in the solar absorptance (from 0.98 to 0.94) and thermal emittance (from 0.31 to 0.30). During these stagnation tests, average daytime plate temperatures ranging from 60 to 100° C were recorded.

## 4.2. Microstructural analysis

Previous X-ray analysis of copper oxide coatings has shown that the coating consists of both cupric (CuO) as well as cuprous ($Cu_2O$) oxide [4]. When the coating is observed during growth using SEM and RED, a progression from a relatively smooth epitaxial cuprous oxide film to a flaky, cupric oxide film is observed (Fig. 5). This transition is evident from previous RED results [8] which showed the copper substrate spot pattern to change into an oriented ring pattern to a spotty CuO pattern, characteristic of fully grown black copper films. Ion milling of this film, on the other hand, showed that there was indeed a dense underlying cuprous oxide film which supported a very porous and fragile surface structure [8].

During heat treatment, the surface morphology and surface RED patterns of black copper coatings were not seen to change [12] (Fig. 6). Only an increase in the thickness of the dense oxide layer close to the substrate was observed (Figs 7a to c) while the total coating thickness remained at approximately 1.0 $\mu$m.

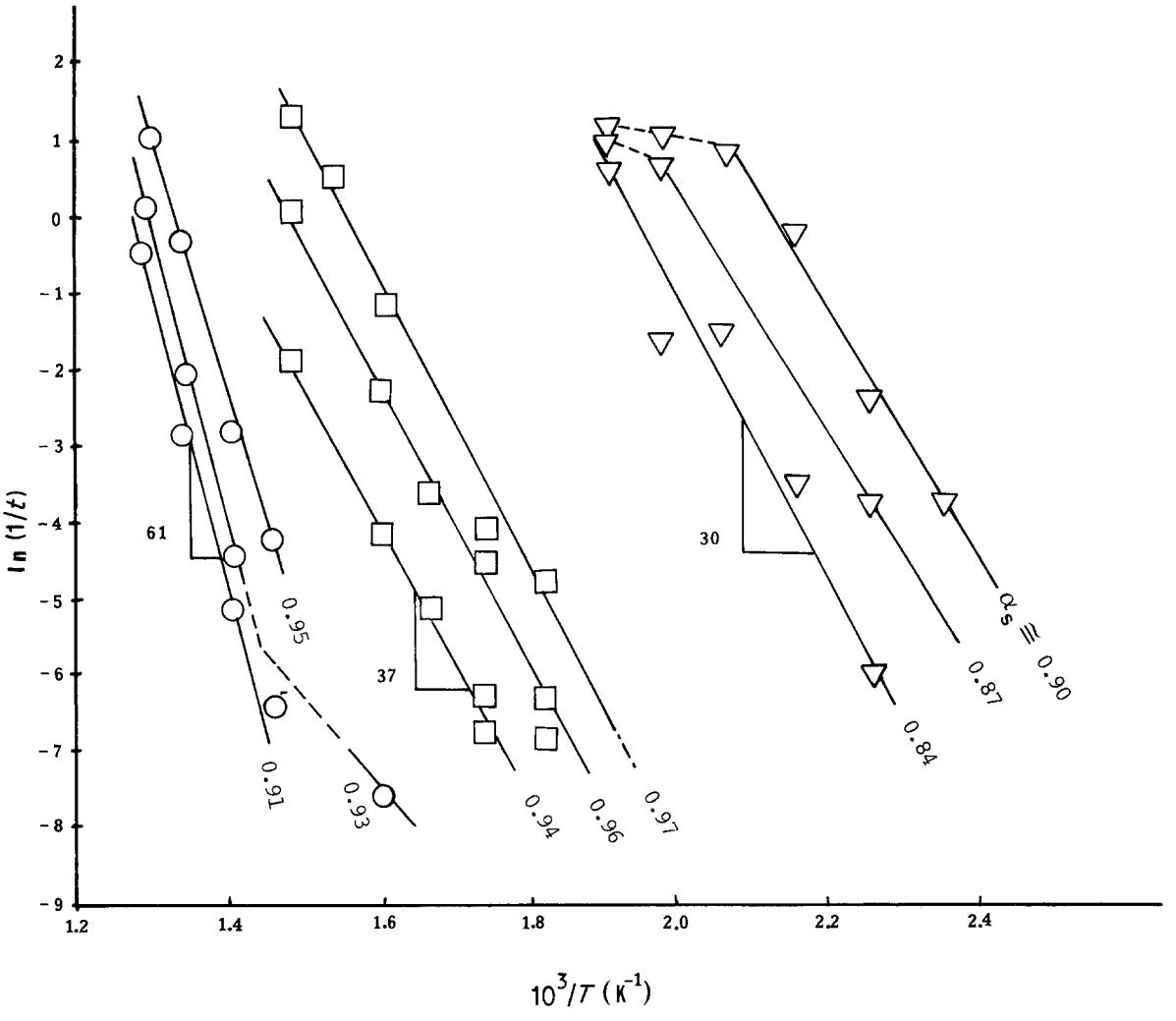


*Figure 2* Arrhenius plot of log (time) of exposure necessary to attain a specified solar absorptance ($\alpha_s$) against inverse temperature for (▽) black copper, (□) black zinc, (○) black chrome.

These observations indicate that the coating degradation appears to occur through the formation of a thicker, dense oxide layer near the substrate at the expense of the porous outer oxide layer.

Auger electron spectroscopy (AES) sputter profiles of this coating show a smooth increase in the copper signal to one that is characteristic of the copper substrate after approximately 30 min of sputtering. There are no indications of any abrupt oxygen signal intensity changes which might result from stoichiometric changes in the oxide composition during sputtering (Fig. 8). Furthermore, there is no detectable difference between AES profiles taken from as-plated and heat-treated black copper samples. This observation also indicates that the total thickness of the coating did not change significantly during degradation.

## 4.3. Optical data for copper and copper oxide

Data for the complex index of refraction ($\tilde{n} = n - ik$) of copper are tabulated by Ordall *et al.* [13] and in the AIP handbook [14] and are displayed in Table I. Optical properties for both cupric and cuprous oxide have previously been determined for wavelengths below 700 nm, where the optical properties of these two oxides are quite similar. Above 700 nm, optical data were calculated from a publication by Prevot *et al.* [15]. As can be seen, these oxides show a characteristic absorption edge at approximately 650 nm (or 2.1 eV). Because

TABLE I Optical properties of copper and copper oxide (either cuprous or cupric oxide)

| Wavelength (nm) | Copper | | Copper oxide | |
|---|---|---|---|---|
| | $n$ | $k$ | $n$ | $k$ |
| 300 | 1.05 | 1.80 | 3.30 | 1.35 |
| 350 | 1.07 | 2.10 | 3.30 | 1.35 |
| 400 | 1.08 | 2.30 | 3.20 | 1.35 |
| 450 | 1.05 | 2.60 | 3.10 | 1.35 |
| 500 | 1.00 | 2.70 | 2.97 | 1.11 |
| 550 | 0.60 | 2.75 | 2.87 | 0.94 |
| 600 | 0.30 | 3.25 | 2.82 | 0.85 |
| 650 | 0.20 | 3.95 | 2.78 | 0.75 |
| 700 | 0.21 | 4.25 | 2.75 | 0.00 |
| 750 | 0.25 | 4.75 | 2.72 | 0.00 |
| 800 | 0.25 | 5.10 | 2.70 | 0.00 |
| 900 | 0.29 | 5.90 | 2.69 | 0.00 |
| 1000 | 0.33 | 6.50 | 2.67 | 0.00 |
| 1100 | 0.38 | 7.40 | 2.65 | 0.00 |
| 1200 | 0.43 | 8.10 | 2.63 | 0.00 |
| 1300 | 0.50 | 8.75 | 2.61 | 0.00 |
| 1400 | 0.58 | 9.60 | 2.61 | 0.00 |
| 1500 | 0.67 | 10.3 | 2.60 | 0.00 |
| 1600 | 0.75 | 11.0 | 2.60 | 0.00 |
| 1700 | 0.85 | 11.8 | 2.60 | 0.00 |
| 1800 | 0.97 | 12.6 | 2.60 | 0.00 |
| 1900 | 1.05 | 13.3 | 2.60 | 0.00 |
| 2000 | 1.17 | 14.0 | 2.60 | 0.00 |
| 2100 | 1.27 | 14.7 | 2.60 | 0.00 |
| 2200 | 1.37 | 15.4 | 2.60 | 0.00 |
| 2300 | 1.50 | 16.3 | 2.60 | 0.00 |
| 2400 | 1.62 | 16.9 | 2.60 | 0.00 |

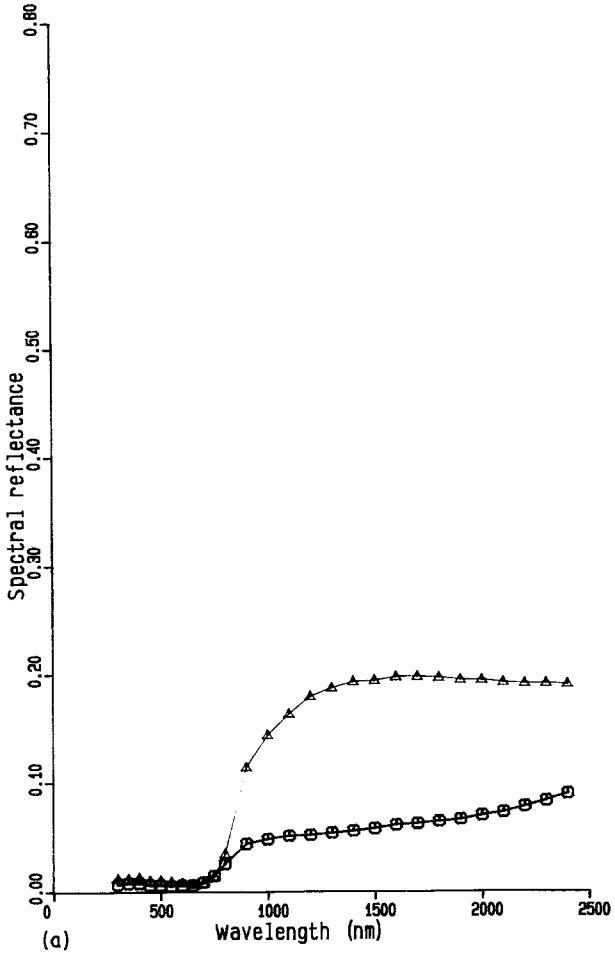


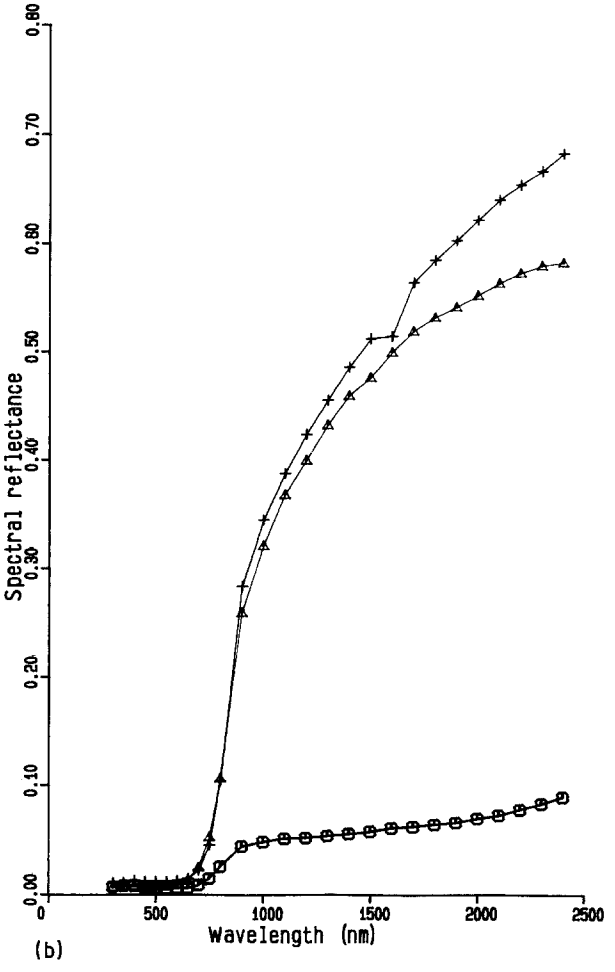


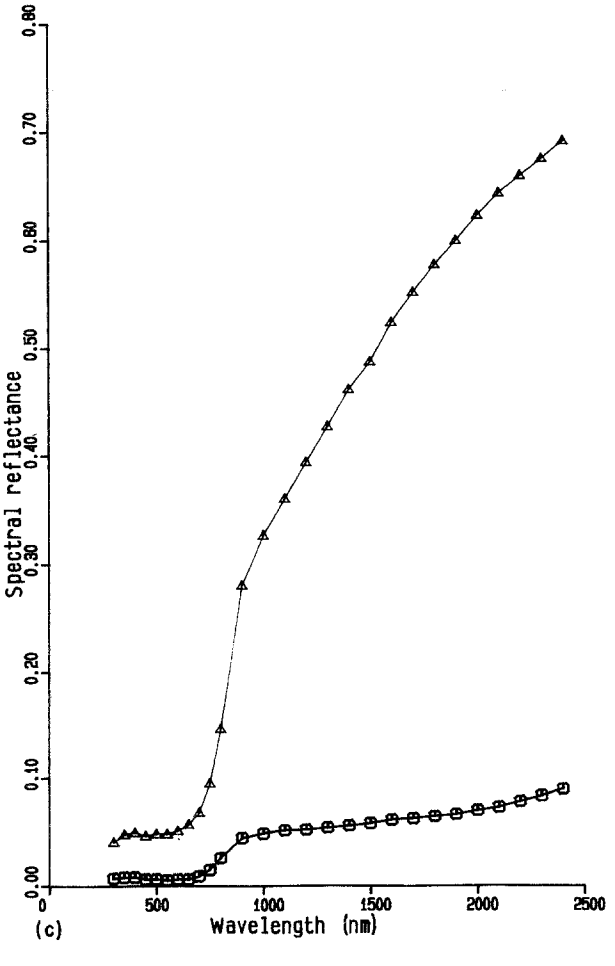


*Figure 3* Measured spectral reflectance curves of black copper during exposure at different temperatures. (a) 150° C: (□) as-plated, (△) 18 h exposure. (b) 205° C: (□) as-plated, (△) 128 h exposure, (+) 2258 h exposure. (c) 250° C: (□) as-plated, (△) 16 h exposure.

of the similarity in optical properties, no distinction needs to be made between the type of oxide that is present for modelling purposes. Therefore the oxide in the optical model will be represented using the symbol $Cu_xO$.

## 4.4. Structural model

The model used to reproduce the measured spectral reflectance behaviour shown in Fig. 3 consisted of a three-layer arrangement. A dense oxide layer, containing metallic copper inclusions, is closest to the substrate. The metallic copper in this layer represents inclusions of copper from the substrate due to microroughness at this interface. The copper volume-fraction gradient in this layer changes linearly from 100% at the substrate–oxide interface to 0% at the top of this first layer. The second layer consists of an optional pure cuprous oxide layer, which in turn supports a third layer which has a "flake-like" surface microstructure as seen in SEM micrographs (Fig. 9). This outer porous surface layer can be modelled as a layer of copper oxide dispersed in air, where the oxide volume fraction varies linearly from 100% $Cu_xO$ at the bottom of the layer to 0% at the oxide–air interface. The needle-like shape of the oxide particles in this layer can be reproduced by including a large aspect ratio of height $c$ to diameter $a$ ($c/a = 5$) in

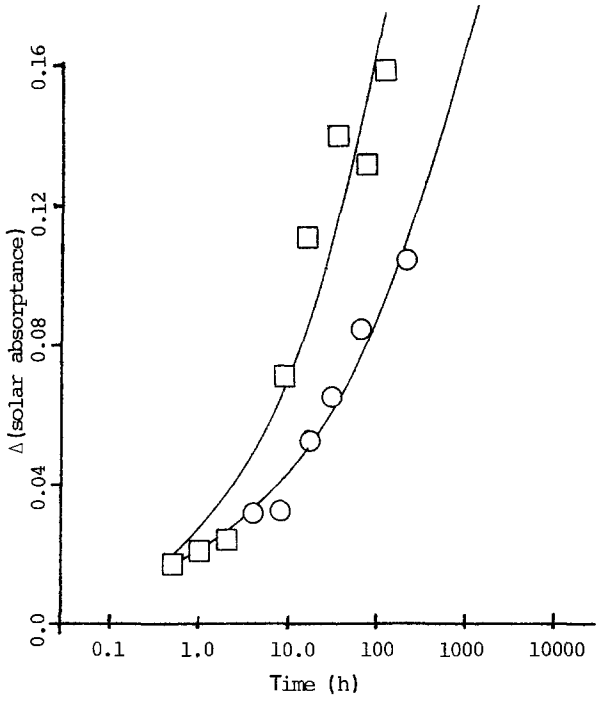


*Figure 4* Change in the solar absorptance against heat treatment time at 150° C: (□) with water-saturated environment, (○) in muffle furnace.

the Maxwell–Garnett calculations. In calculating the effective dielectric constant of this layer, the long axis of the oxide particles was orientated perpendicular to the substrate and thus parallel to the incident beam direction.

When measured microstructural details are introduced into this structural model for black copper, the following optimum film parameters are found to reproduce the as-plated reflectance properties (see Fig. 10):

| | | |
|---|---|---|
| 1. | Cu–$Cu_xO$ thickness | 0.5 $\mu$m |
| | $c/a$ ratio of copper particles | 1.0 |
| | Gradient of copper in oxide | Linear |
| 2. | $Cu_xO$ thickness (optional) | 0.0 $\mu$m |
| 3. | $Cu_xO$–air thickness | 0.3 $\mu$m |
| | $c/a$ ratio of $Cu_xO$ particles | 5.0 |
| | Gradient of $Cu_xO$ in air | Linear |

The reflectance characteristics as a function of the outer $Cu_xO$–air layer thickness are also shown in Fig. 10. Note that decreasing the thickness of this layer increases the reflectance both above and below the absorption band (650 nm). A thickness of $\approx 0.3\,\mu$m appears to provide a good replication of the reflectance characteristics of the experimental curve.

Reproducing the reflectance behaviour after thermal ageing involves a simultaneous decrease in the outer $Cu_xO$–air layer thickness and an increase in the Cu–$Cu_xO$ layer thickness, such that the total coating thickness remains unchanged. Calculated reflectance curves are shown in Fig. 11 for Cu–$Cu_xO$ layer thicknesses from 0.3 to 1.2 $\mu$m with the $Cu_xO$–air layer thickness fixed at 0.1 $\mu$m. As can be seen, decreasing the $Cu_xO$–air layer thickness from 0.3 to 0.1 $\mu$m increases the reflectance above 650 nm, while changing the thickness of the Cu–$Cu_xO$ layer from 0.8 to 1.2 $\mu$m has little additional effect on the calculated reflectance curves. The increase in reflectance calculated at wavelengths below the absorption edge is, in this case, considered to be an artefact of the model, attributable to the abrupt changes in the refractive index between layers of the oxide close to the absorption band. Therefore, decreasing the $Cu_xO$–air layer thickness from 0.3 to 0.1 $\mu$m and increasing the Cu–$Cu_xO$ layer thickness from 0.5 to 0.7 $\mu$m provides a reasonable match to the experimentally measured reflectance properties after thermal ageing.

The inclusion of a pure $Cu_xO$ layer between the two

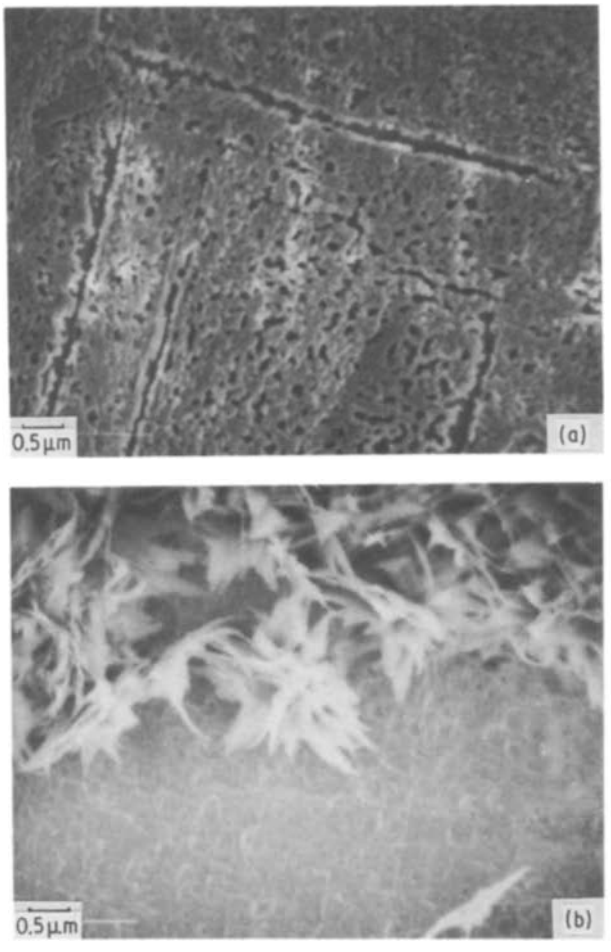


*Figure 5* (a) SEM micrograph of smooth epitaxial layer formed after 30 sec of chemical oxidation during growth of black copper. (b) Black copper layer after 180 sec of chemical oxidation. (c) Black copper after 360 sec of chemical oxidation.

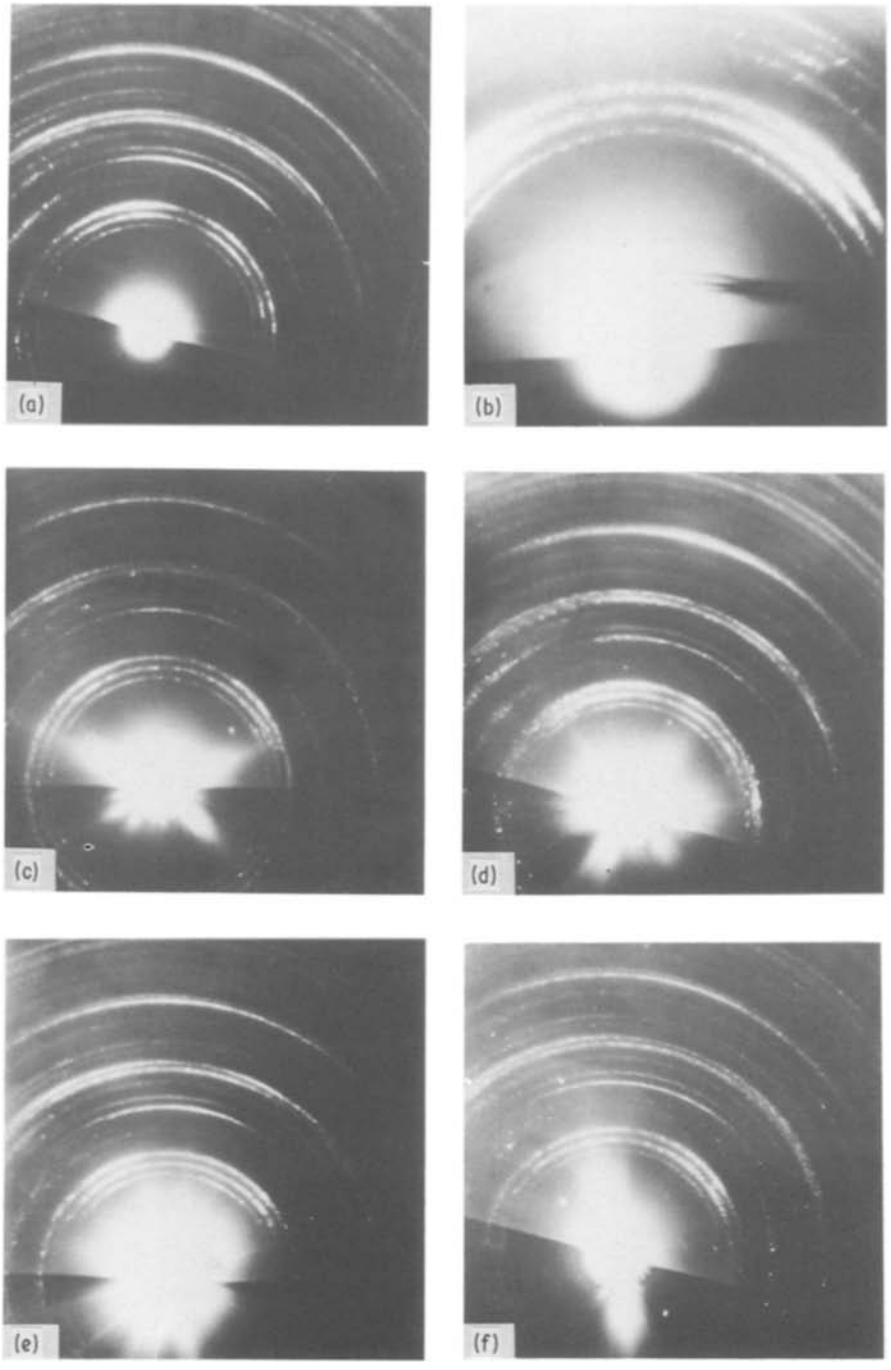


*Figure 6* (a) As-coated black copper RED pattern at 100 kV electron beam potential. (b) As-coated black copper RED pattern at 50 kV. (c–f) RED patterns of black copper after heat treatment at 205° C for (c) 0.5, (d) 1, (e) 8, (f) 16 h.

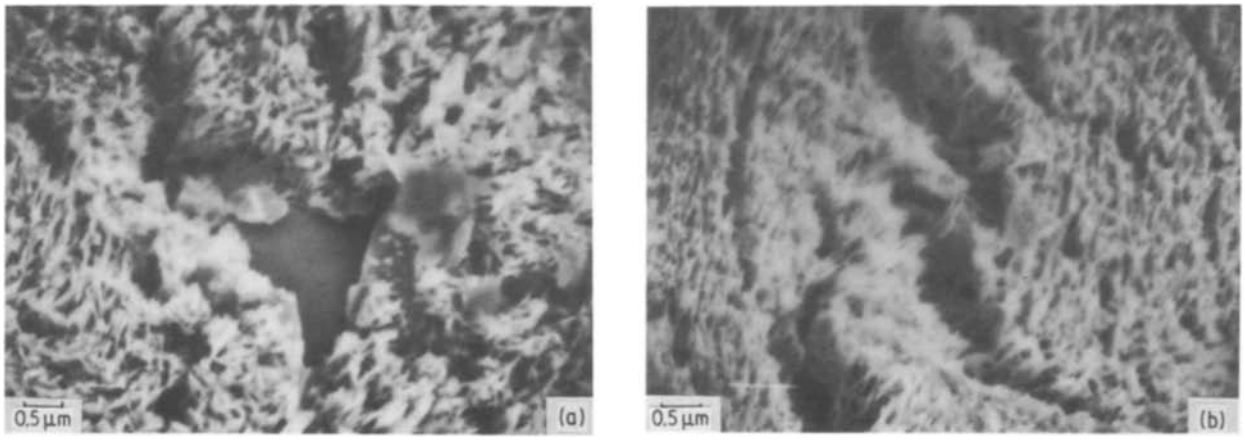


*Figure 7* SEM micrograph of black copper (a) as-plated showing fractured layer, (b) after 30 min at 205° C, (c) after 64 h at 205° C.

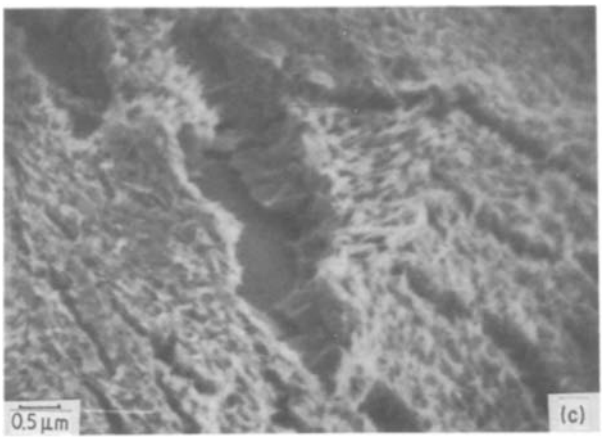


*Figure 7* Continued

graded layers did not provide a better match with the degraded reflectance properties, as shown in Fig. 12. In addition, changes in the gradient of the metallic copper in the Cu–$Cu_xO$ layer to a higher power law, as well as changing the $c/a$ ratio, did not enhance the fit of the model to the measured reflectance properties. Therefore, after heat treatment, the spectral reflectance behaviour is best reproduced by the following coating parameters:

| | | |
|---|---|---|
| 1. | Cu–$Cu_xO$ thickness | 0.7 μm |
| | $c/a$ ratio of copper particles | 1.0 |
| | Gradient of copper in oxide | Linear |
| 2. | $Cu_xO$ thickness | 0.0 |
| 3. | $Cu_xO$–air thickness | 0.1 μm |
| | $c/a$ ratio of $Cu_xO$ particles | 5.0 |
| | Gradient of $Cu_xO$ in air | Linear |

Therefore, a decrease in the roughness of the outer surface layer, from 0.3 to 0.1 μm, increases the surface reflection losses and gives rise to the degradation that is observed even at low temperatures. If this change is accompanied by a corresponding increase in the dense oxide thickness, the measured spectral reflectance changes can be successfully reproduced by the structural model.

## 5. Discussion and conclusions

The two principal objectives pursued by this study were to characterize the structural changes in copper oxide coatings as a result of thermal exposure and to determine the ageing behaviour of the coatings as a function of time and temperature of exposure.

The internal structure of black copper deposits has

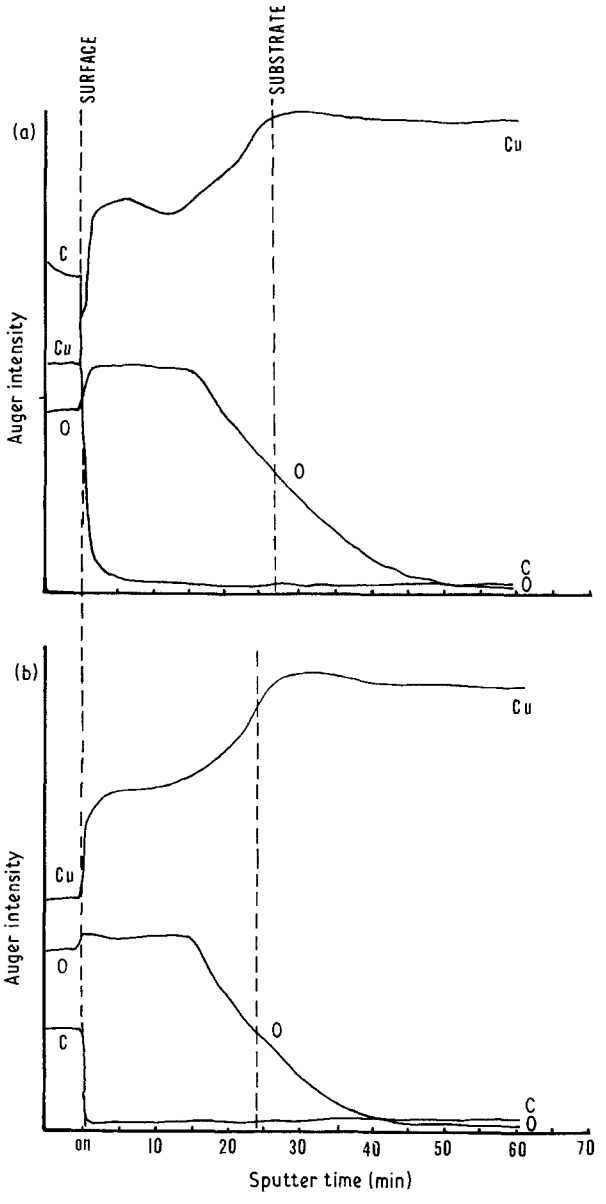


*Figure 8* AES sputter profile of (a) as-plated black copper, (b) black copper after exposure to 205° C for 128 h.

previously been described by Milgram [7] through the use of qualitative analysis of the reflectance against wavelength response. The unique surface geometries of these coatings were thought to contribute significantly to the high solar absorptance values inherent in the as-deposited black copper deposits.

The present study has described the coating structures more quantitatively, with the Maxwell–Garnett theory, and approximated the effect of the outer surface roughness as well as the roughness at the oxide–

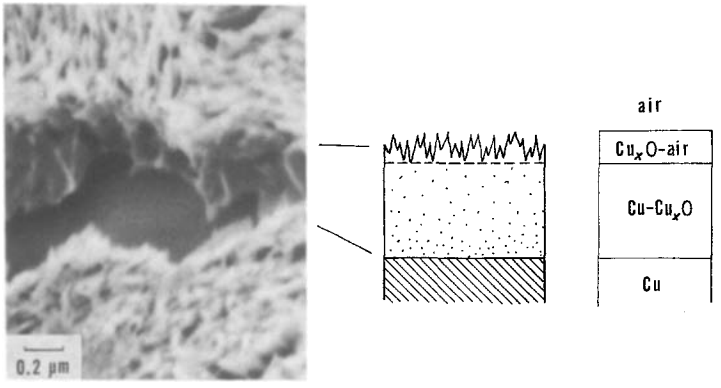


*Figure 9* SEM micrograph and schematic diagram of film structure used in the optical model.

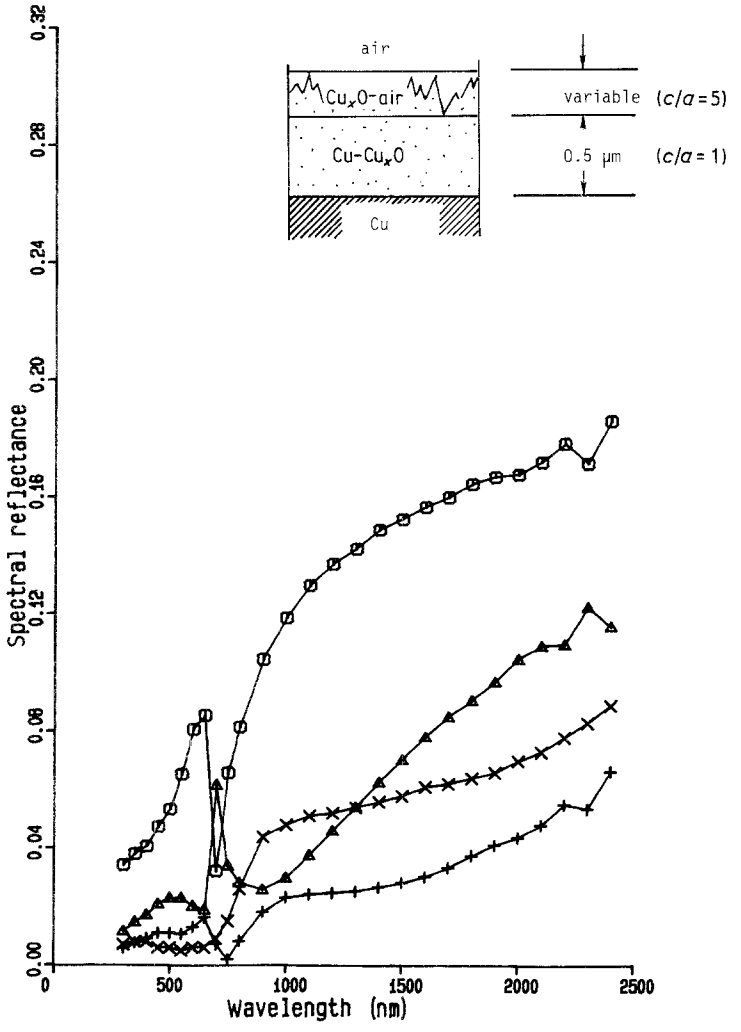


*Figure 10* Effect of changing the outer $Cu_xO$–air layer thickness from 0.1 to 0.3 $\mu$m on the calculated reflectance properties for as-plated films: (□) 0.1 $\mu$m $Cu_xO$–air, (△) 0.2 $\mu$m $Cu_xO$–air, (+) 0.3 $\mu$m $Cu_xO$, (x) measured as-plated.

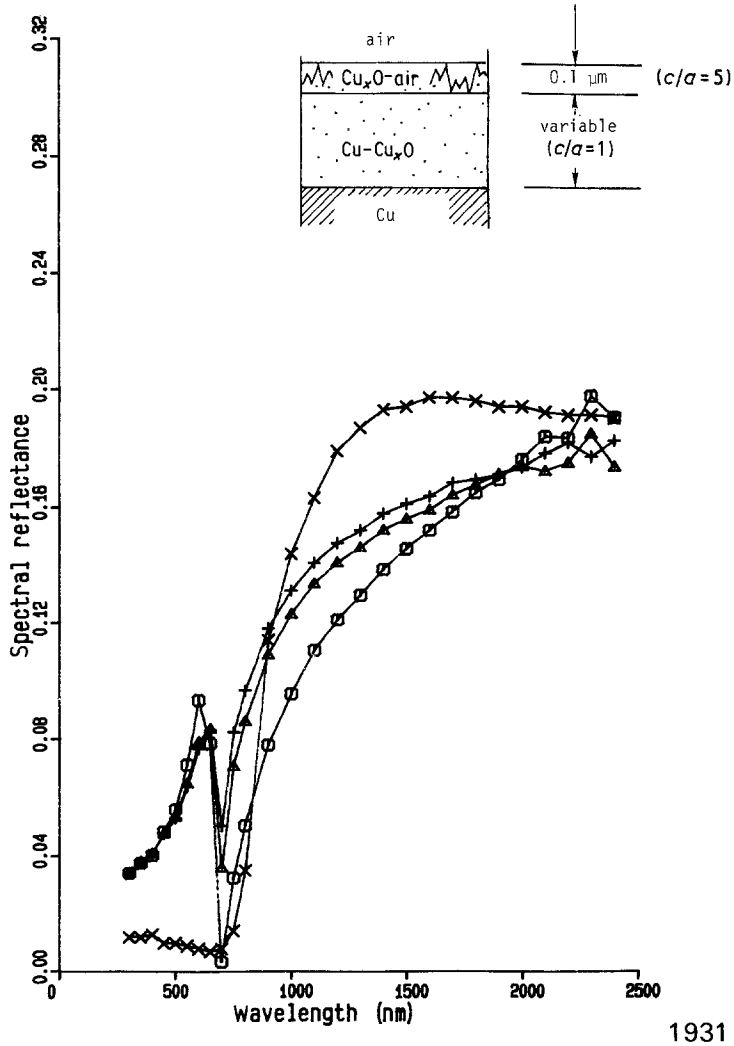


*Figure 11* Effect of changing the thickness of the Cu–$Cu_xO$ layer on the calculated reflectance properties after thermal ageing: (□) 0.3 $\mu$m Cu–$Cu_xO$, (△) 0.8 $\mu$m Cu–$Cu_xO$, (+) 1.2 $\mu$m Cu–$Cu_xO$, (x) measured, after 18 h at 150° C.

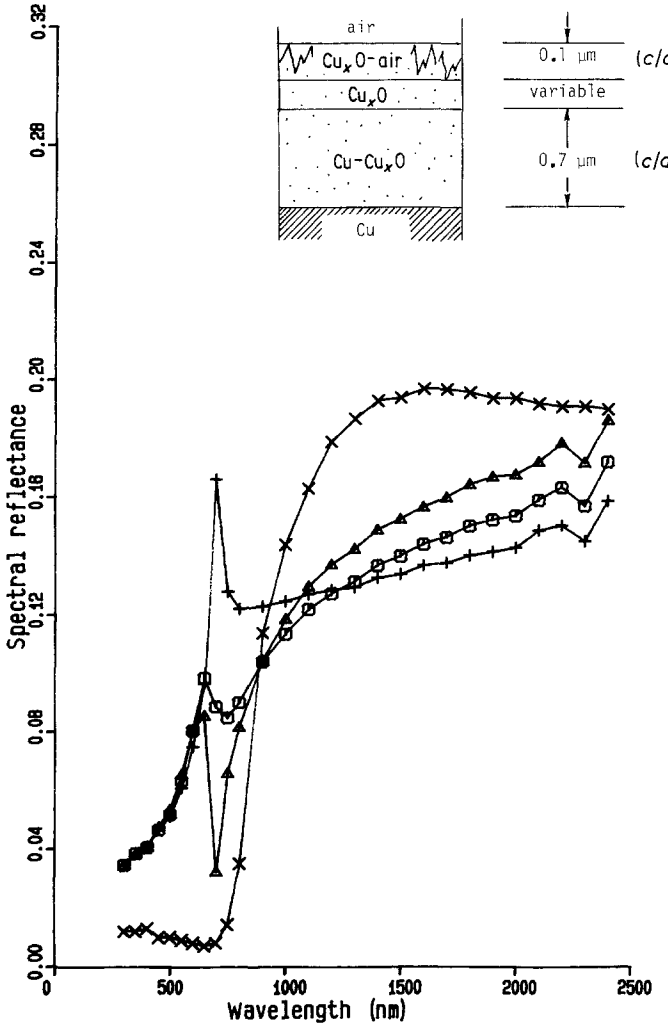


*Figure 12* Effect of including a dense copper oxide layer between the Cu–$Cu_xO$ and $Cu_xO$–air layers on the reflectance properties after thermal ageing: (△) no $Cu_xO$, (□) 0.02 μm $Cu_xO$, (+) 0.04 μm $Cu_xO$, (×) measured after 18 h at 150° C.

substrate interface. A two-layer film was found to reproduce the as-plated reflectance against wavelength behaviour. This film consisted of a graded layer of oxide containing copper, which supported the rough oxide surface layer. The heat-treated structure of black copper was best matched with a thicker Cu–$Cu_xO$ layer and a correspondingly thinner $Cu_xO$–air layer. Degradation is therefore thought to occur initially through a decrease in the thickness of the $Cu_xO$–air layer dimension (from 0.3 to 0.1 μm), and later through an increase in the Cu–$Cu_xO$ layer thickness (at higher temperatures and/or longer times). This degradation is accelerated in humid environments.

In conclusion, this study has determined a degradation mechanism, supported by microstructural analysis and optical modelling, for black copper. It was found that, provided detailed microstructural data are available, confidence can be placed in the optically derived coating models for these oxide layers. Such models of coating microstructures and their changes during degradation were found to be essential in the prediction of long-term degradation behaviour.

## Acknowledgements

The authors are indebted to Mr J. L. Rife of Sandia National Laboratories, who obtained the Auger electron spectroscopy sputter profiles for this study. This research was funded in part by the US Department of Energy, under Division of Materials Science Contract No. DE-ER-78-04-4266, which is gratefully acknowledged. Portions of this work performed at Sandia National Laboratories were also supported by the US Department of Energy, under Contract No. DE-AC04-76-DP00789.

## References

1. R. D. PATEL, M. G. TAKWALE, V. K. NAGAR and V. G. BHIDE, *Thin Solid Films* **115** (1984) 169.
2. A. A. MILGRAM, *J. Appl. Phys.* **54** (1983) 1053.
3. J. N. SWEET, R. B. PETTIT and M. B. CHAMBERLAIN, *Solar Energy Mater.* **10** (1984) 36.
4. O. T. INAL and A. SCHERER, *J. Mater. Sci.* **21** (1986) 729.
5. A. SCHERER, O. T. INAL and A. J. SINGH, *Solar Energy Mater.* **9** (1983) 139.
6. L. W. MASTERS, J. F. SEILER, E. J. EMBREE and W. E. ROBERTS, "Solar Energy Systems–Standards for Absorber Materials", US DOC NBSIR 81-2232 (1981).
7. A. A. MILGRAM, *J. Appl. Phys.* **54** (1983) 3640.
8. A. SCHERER and O. T. INAL, *Thin Solid Films* **119** (1984) 413.
9. O. S. HEAVENS, "Optical Properties of Thin Solid Films" (Dover, New York, 1965) p. 141.
10. H. G. CRAIGHEAD and R. A. BUHRMAN, *J. Vac. Sci. Technol.* **15** (1978) 269.
11. N. H. NIE, C. HADLAIHULL, J. JENKINS, K. STEINBRENNER and D. BENT, "Statistical Package for the Social Sciences" (McGraw-Hill, New York, 1975).
12. A. SCHERER and O. T. INAL, *Thin Solid Films* **121** (1984) 279.
13. M. A. ORDALL, L. L. LONG, R. J. BELL, S. E.

BELL. R. R. BELL, R. W. ALEXANDER JR and C. A. WARD, *Appl. Opt.* **22** (1983) 1099.
14. D. E. GRAY (ed.), "American Institute of Physics Handbook", 3rd. Edn (McGraw-Hill, New York, 1972), pp. 6-124 to 6-155.
15. B. PREVOT, C. CARABATOS and M. SIESKIND, *Phys. Status Solidi* (*a*) **10** (1972) 455.

*Received 3 November*
*and accepted 28 January 1987*